The Journal of the Astronautical Sciences, Vol. 32, No. 4, October-December 1984, pp. 429–445.

Second-Order Analytic Solutions for Aerocapture and Ballistic Fly-Through Trajectories[1]

**Nguyen X. Vinh,[2] Jennie R. Johannesen,[2]
James M. Longuski,[3] and John M. Hanson[4]**

Abstract

Future missions may involve the use of aerocapture for planetary exploration and atmospheric braking for aeroassisted orbital transfers. When only one pass through the atmosphere is considered to deplete the speed to the desired value at exit, the exit conditions are very sensitive to the entry angle. Near a certain critical entry angle, a slight modification of the entry angle may change a skip trajectory into a crashing trajectory. In this paper, we have derived a generalized Yaroshevskii's system of equations for analyzing ballistic entry at super-circular speeds. Then, by an artifical introduction of a small parameter, the nonlinear system can be integrated by Poincaré's method. The second-order theory displays explicitly the influence of the ballistic coefficient, entry speed and entry angle on exit conditions. The analytic solution is in excellent agreement with the numerical solution. The critical entry angle at which the vehicle fails to skip out can be predicted by an explicit formula to within one hundredth of a degree.

Introduction

When an orbital maneuver is required and there is an atmosphere-bearing celestial body in the vicinity, it may be advantageous to utilize aerodynamic force in effecting the maneuver to reduce the fuel consumption as compared to the cost for a purely propulsive maneuver. Examples of aeroassisted transfer include orbital transfer from a high orbit to a low orbit with or without plane change, and aerogravity capture to put a spacecraft into an orbit around a distant planet. A comprehensive survey of aeroassisted orbital transfer has been presented by Walberg [1].

The operation always includes one phase of atmospheric fly-through along which the speed of the vehicle is reduced from an initial entry speed V_e to a final exit speed V_f,

[1]Presented at the AAS/AIAA Astrodynamics Conference, Lake Placid, New York, August 22–25, 1983.
[2]Department of Aerospace Engineering, The University of Michigan, Ann Arbor, MI 48109-2140.
[3]Jet Propulsion Laboratory, Pasadena, CA 91109.
[4]Analytic Services, Inc., Arlington, VA 22202.

while the flight path angle varies from a negative value, γ_e, to a positive value, γ_f. An accurate prediction of the final values, V_f and γ_f, is important for guidance and navigation purposes and also for an evaluation of the characteristic velocity involved in the overall aeroassisted maneuver.

It is the purpose of this paper to present an analytic investigation of this important skip phase for the case of constant ballistic coefficient. Extensive numerical investigation has been carried out for this type of ballistic skip trajectory with and without drag modulation [2]. With only the drag force involved and with the effect of the rotation of the atmosphere neglected, the motion is planar.

For constant ballistic coefficient, the following phenomena have been observed. The speed ratio, V_f/V_e, decreases as the drag parameter, SC_D/m, increases. Here S, C_D, and m are the reference area, drag coefficient and mass of the vehicle, respectively. The speed ratio also decreases when the entry speed decreases. The dependence of the exit condition on the entry angle is pronounced. For a shallow entry trajectory the exit speed is high, while the exit angle is nearly equal to the negative of the entry angle. As the entry angle becomes steeper, the exit speed is significantly reduced for the same drag parameter and entry speed.

Near a critical entry angle γ_e^*, the exit angle decreases rapidly to grazing exit, $\gamma_f = 0$. The ballistic trajectory is sensitive to change near this critical value. With a slight modification of the entry angle, the trajectory may change from a skip trajectory to a crashing trajectory (Fig. 1).

Since, in optimal aeroassisted transfer, a shallow exit trajectory will reduce the characteristic velocity for orbit insertion, it is of interest to have accurate analytic expressions for the exit variables as functions of the entry conditions and drag parameter. Once this dependence is made explicit through pertinent analytic formulas and the phenomena mentioned above are clearly understood, an optimal strategy for adaptive guidance of a ballistic skip trajectory can be soundly formulated.

In the following sections we will transform the equations of motion into dimensionless form and integrate these equations using Poincaré's method of small parameters to arrive at a second-order analytical solution for the altitude and flight path angle variables. These analytic solutions will then be compared with the results from numerical integration for both shallow entry angles and entry near the critical angle.

Dimensionless Equations

Using the standard notation with r for radial distance, V for speed, t for time, ρ for atmospheric density and g for gravitational acceleration, we have the following planar equations of motion for flight inside the atmosphere of a non-rotating planet.

$$dr/dt = V \sin \gamma \tag{1}$$

$$dV/dt = -\rho S C_D V^2/(2m) - g \sin \gamma \tag{2}$$

$$V\, d\gamma/dt = -(g - V^2/r) \cos \gamma \tag{3}$$

The atmosphere is assumed to be locally exponential according to the relation

$$d\rho = -\beta(r)\rho\, dr \tag{4}$$

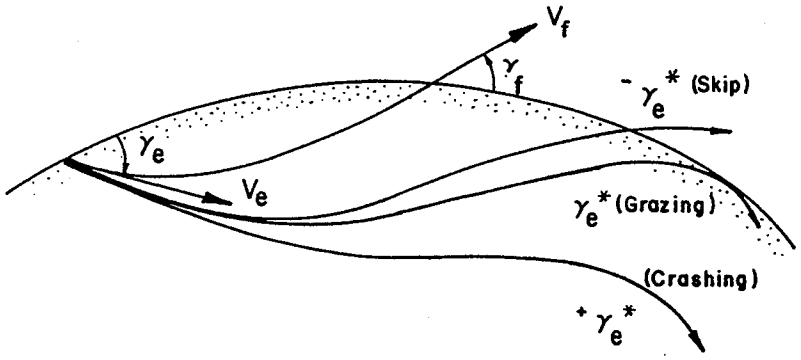

FIG. 1. Geometry of Ballistic Skip Trajectory with Behavior Near Critical Entry Angle, γ_e^*.

where β is the inverse scale height. Using R as the radius of the atmosphere, we make the assumption $g(r) \approx g(R)$ and $V^2/r \approx V^2/R$. It can be shown that the error committed by this assumption is of the same order as the one committed while neglecting the Coriolis force associated with a rotating Earth. Furthermore, for a flight path angle of only a few degrees, we neglect the small component of the gravitational acceleration, $-g \sin \gamma$. This is invariably the case in the present study since the critical entry angle γ_e^*, which is the steepest flight path angle, is always small.

By using the variables

$$Z = \rho S C_D m^{-1} (R/\beta)^{1/2} \tag{5}$$

$$\phi = -(\beta R)^{1/2} \sin \gamma \tag{6}$$

$$x = \log(V_c^2/V^2) \tag{7}$$

to denote the altitude, flight path angle and speed, respectively, and the parameter α, given by

$$\alpha = gR/V_c^2 = V_c^2/V_c^2 \tag{8}$$

we can transform the equations of motion into dimensionless form as

$$dZ/dx = \phi \tag{9}$$

$$d\phi/dx = (\alpha e^x - 1) Z^{-1} \cos^2 \gamma \tag{10}$$

where the equations corresponding to equations (1) and (3) have been divided by equation (2) to remove the time. Consistent with the small angle approximation, we integrate the equations in the form

$$dZ/dx = \phi \tag{11}$$

$$d\phi/dx = (\alpha e^x - 1) Z^{-1} \tag{12}$$

with the initial conditions

$$x = 0, \qquad Z(0) = \varepsilon = \rho_e S C_D m^{-1} (R/\beta)^{1/2}, \qquad \phi(0) = -(\beta R)^{1/2} \sin \gamma_e = c \tag{13}$$

We notice that x is the speed variable and is monotonically increasing, while ε is the dimensionless drag parameter. The effect of the entry angle is denoted by the value

$c > 0$. In equation (8) the effect of the entry speed is represented by the parameter α, with $\alpha = 0.5$ for parabolic entry and increasing to $\alpha = 1$ for circular entry. Of course, when $\alpha < 0.5$ we have hyperbolic entry which is applicable to the case of planetary aerocapture. The parameter βR is Chapman's atmospheric planetary parameter and for the Earth's atmosphere it has the value $\beta R = 900$. In deriving the equation for Z we have used a varying β. By neglecting a quantity of the order of $1/\beta R$ we have the resulting equation which is the same as if β had been considered as constant. Discussion of this rather subtle point can be found in [3]. Equations (11) and (12) constitute the generalized Yaroshevskii's equations for supercircular ballistic entry [4]. It has been verified numerically that for circular entry ($\alpha = 1$) the numerical integration of equations (11) and (12) provides nearly identical results as compared to the numerical solution of the exact equations (1)-(3) [5]. This has also been verified for the case of parabolic entry ($\alpha = 0.5$). Hence, in the following we shall integrate analytically the system (11), (12) and compare the results with its numerical solution.

The simplest way to integrate the generalized Yaroshevskii's equations is to use the conventional power series solutions. In using this approach, however, the radius of convergence of the series is small and the solution obtained is designed for use with small variations in the speed. To extend the range of validity of the solution, we shall use Poincaré's method by artificially inserting a small parameter. For this purpose, we make the final change of variables

$$y = Z/\varepsilon, \qquad \tau = x/\varepsilon, \qquad d(\ )/d\tau = (\ )' \tag{14}$$

to obtain the equations

$$y' = \phi, \qquad \phi' = (\alpha e^{\varepsilon\tau} - 1)/y \tag{15}$$

with the initial conditions

$$\tau = 0, \qquad y(0) = 1, \qquad \phi(0) = c \tag{16}$$

For the time of flight, we add the uncoupled equation

$$d\theta/d\tau = \alpha^{1/2} e^{\varepsilon\tau/2} y^{-1} \tag{17}$$

where θ is the dimensionless time, given by

$$\theta = (\beta g)^{1/2} t \tag{18}$$

A parameter of interest along the ballistic trajectory is the longitudinal deceleration, which can be expressed as

$$a/g = \varepsilon(2\alpha)^{-1}(\beta R)^{1/2} y e^{-\varepsilon\tau} \tag{19}$$

By maximizing this function we have the relation at the point of peak deceleration

$$\phi = \varepsilon y \tag{20}$$

Expressions can also be found for various heating rates and conditions where the peak heating rates occur.

The altitude variable has been represented by the dimensionless atmospheric density y, normalized with respect to the density at the entry altitude (taken as $h_e = 120$ km). The variation of the linear altitude h is simply

$$\beta(h - h_e) = \beta \Delta h = -\log y \tag{21}$$

Integration by Poincaré's Method

We first integrate equations (15) using Poincaré's method of small parameters. By noticing that the drag parameter ε is of the order of 10^{-3}, we seek solutions of the form

$$y = y_0 + \varepsilon y_1 + \varepsilon^2 y_2 + \cdots \tag{22}$$

$$\phi = \phi_0 + \varepsilon\phi_1 + \varepsilon^2\phi_2 + \cdots \tag{23}$$

with the initial conditions

$$y_0(0) = 1, \qquad y_1(0) = y_2(0) = \cdots = 0 \tag{24}$$

$$\phi_0(0) = c, \qquad \phi_1(0) = \phi_2(0) = \cdots = 0 \tag{25}$$

Upon substituting into equations (15) and equating coefficients of like powers in ε, we have the systems of equations

$$y_0' = \phi_0 \tag{26}$$

$$\phi_0' = -(1 - \alpha)/y_0 \tag{27}$$

$$y_1' = \phi_1 \tag{28}$$

$$\phi_1' = (1 - \alpha)y_1/y_0^2 + \alpha\tau/y_0 \tag{29}$$

$$y_2' = \phi_2 \tag{30}$$

$$\phi_2' = (1 - \alpha)y_2/y_0^2 - \alpha\tau y_1/y_0^2 + \alpha\tau^2/2y_0 - (1 - \alpha)y_1^2/y_0^3 \tag{31}$$

For the zeroth order solution, we write the equation

$$dy_0/d\phi_0 = -y_0\phi_0/(1 - \alpha) \tag{32}$$

which, upon integration, provides the variation of the altitude as a function of the flight path angle

$$y_0 = \exp[(c^2 - \phi_0^2)/\delta] \tag{33}$$

where, for convenience of notation, we have put

$$\delta = 2(1 - \alpha) \tag{34}$$

The speed, which is represented by the variable τ, is found by substituting for y_0 from equation (33) into equation (27), which upon integration provides

$$\tau = (\pi/\delta)^{1/2} \exp(c^2/\delta)[\operatorname{erf}(c\delta^{-1/2}) - \operatorname{erf}(\phi_0\delta^{-1/2})] \tag{35}$$

Here the error function, which is a tabulated function [6], is defined to be

$$\operatorname{erf}(x) = 2\pi^{-1/2}\int_0^x e^{-t^2}\,dt \tag{36}$$

The zeroth order solution is adequate for high-speed entry, where the parameter α is not near unity, with shallow flight path angle. The vehicle exits when $y_0 = 1$, and as a consequence, in this approximation the exit angle is equal to the negative of the entry angle, that is, $\phi_f = -c$.

To include the effect of variation of the speed, we consider the first order system equations (28) and (29), written as

$$y_0^2 y_1'' - (1 - \alpha) y_1 = \alpha y_0 \tau \tag{37}$$

It is easy to verify that the solution of the homogeneous system is

$$y_1 = B_1 \phi_0 + B_2 (y_0 - \phi_0 \tau) \tag{38}$$

$$\phi_1 = -(1 - \alpha) B_1 y_0^{-1} + (1 - \alpha) B_2 \tau y_0^{-1} \tag{39}$$

By varying the parameters B_1 and B_2 and forcing the solution, equations (38) and (39), to satisfy the complete system, equations (28) and (29), we have the equations

$$B_1' = 2\alpha\delta^{-1}(\phi_0 \tau^2 y_0^{-1} - \tau) \tag{40}$$

$$B_2' = 2\alpha\delta^{-1}\phi_0 \tau y_0^{-1} \tag{41}$$

These quadratures can be performed by integration by parts and we now have

$$B_1 = -2\alpha\delta^{-2}(y_0 - \phi_0 \tau)^2 + A_1 \tag{42}$$

$$B_2 = \alpha\delta^{-1}\tau + 2\alpha\delta^{-2}\phi_0 (y_0 - \phi_0 \tau) + A_2 \tag{43}$$

By substituting into equations (38) and (39) and evaluating the constants of integration, A_1 and A_2, using the initial conditions from equations (24) and (25), we have the first order solution

$$y_1 = 2\alpha\delta^{-2}\phi_0 + 2\alpha\delta^{-2} k (y_0 - \phi_0 \tau) \tag{44}$$

$$\phi_1 = \alpha\delta^{-1}(k\tau - 1) y_0^{-1} + \alpha\delta^{-1}(y_0 - \phi_0 \tau) \tag{45}$$

where, by definition,

$$k = (1 - \alpha)\tau - c \tag{46}$$

The integration of the second-order system, equations (30) and (31), is performed in the same way as with the first-order system, equations (28) and (29), but the quadratures involved are much more elaborate. The final results are

$$\begin{aligned} y_2 = {} & 2\alpha\delta^{-3}(y_0 - \phi_0 \tau)[(1 + \alpha) + (1 - \alpha)\tau^2] \\ & + \alpha\delta^{-3}\phi_0 \tau[\alpha + (\delta/6)(\alpha + 2)\tau^2] - \alpha\delta^{-3}(\alpha + 2) y_0^3 \\ & - \alpha^2\delta^{-3}(k\tau - 1)^2 y_0^{-1} + \alpha\delta^{-2} k y_1 \\ & - 6\alpha\delta^{-4}(\alpha + 2)\phi_0 [K(\phi_0) - K(c)] \end{aligned} \tag{47}$$

$$\begin{aligned} \phi_2 = {} & 2\alpha\delta^{-2}(y_0 - \phi_0 \tau)\tau + \alpha\delta^{-3}\phi_0[\alpha + (1 - \alpha)(\alpha + 2)\tau^2] \\ & + (\alpha/6)\delta^{-2}\tau y_0^{-1}[3(\alpha + 2) + (1 - \alpha)(4 - \alpha)\tau^2] \\ & + \alpha^2\delta^{-3}(k\tau - 1)^2 \phi_0 y_0^{-2} + (\alpha/2)\delta^{-1} y_1 + \alpha\delta^{-2} k \phi_1 \\ & - 2\alpha^2\delta^{-3}(k\tau - 1) y_0^{-1}[k + (1 - \alpha)\tau] \\ & + 3\alpha\delta^{-3}(\alpha + 2) y_0^{-1}[K(\phi_0) - K(c)] \end{aligned} \tag{48}$$

where, by definition,

$$K(\phi_0) = (\delta\pi/12)^{1/2} \exp(3c^2/\delta) \operatorname{erf}[(3/\delta)^{1/2}\phi_0] \tag{49}$$

Poincaré's method of integration with a small parameter is a uniformly convergent scheme, but since the equations generated are based on the series expansion of $e^{\varepsilon\tau}$, the solution to the second order is restricted to the range of speed where $\varepsilon\tau$ is small. We notice that if τ_f is the final value, the speed ratio is

$$V_f/V_e = \exp(-x_f/2) = \exp(-\varepsilon\tau_f/2) \tag{50}$$

By the solution for τ, equation (35), with the approximation $\phi_0(\tau_f) = -c$, we can see that a small τ_f requires high speed entry (small α) and a shallow entry angle (small c).

Numerical Example

In the numerical applications of the second-order solution, ϕ_0 is used as the independent variable which monotonically decreases from the initial value c. For each value of ϕ_0 we compute the speed variable τ and subsequently the flight path angle variable ϕ and the altitude variable y.

As an example, we consider the case of parabolic entry, $\alpha = 0.5$, with a ballistic parameter $\varepsilon = 0.0005$. The exact numerical integration of equations (15) has been performed using various entry angles $\gamma_e = -1°, -2°$, etc. The results are presented in Figs. 2 through 5.

Figure 2 presents the variations of the dimensionless linear altitude, $\beta\,\Delta h = -\log y$, as a function of the flight path angle for the case of small entry angles, $-\gamma_e \leq 3°$. As expected in this case the second-order solution is very accurate. To the accuracy of the plot we have simply used the zeroth order solution. By equation (33), this simple analytic solution represents in the space $(\gamma, \beta\,\Delta h)$ the trajectories as a

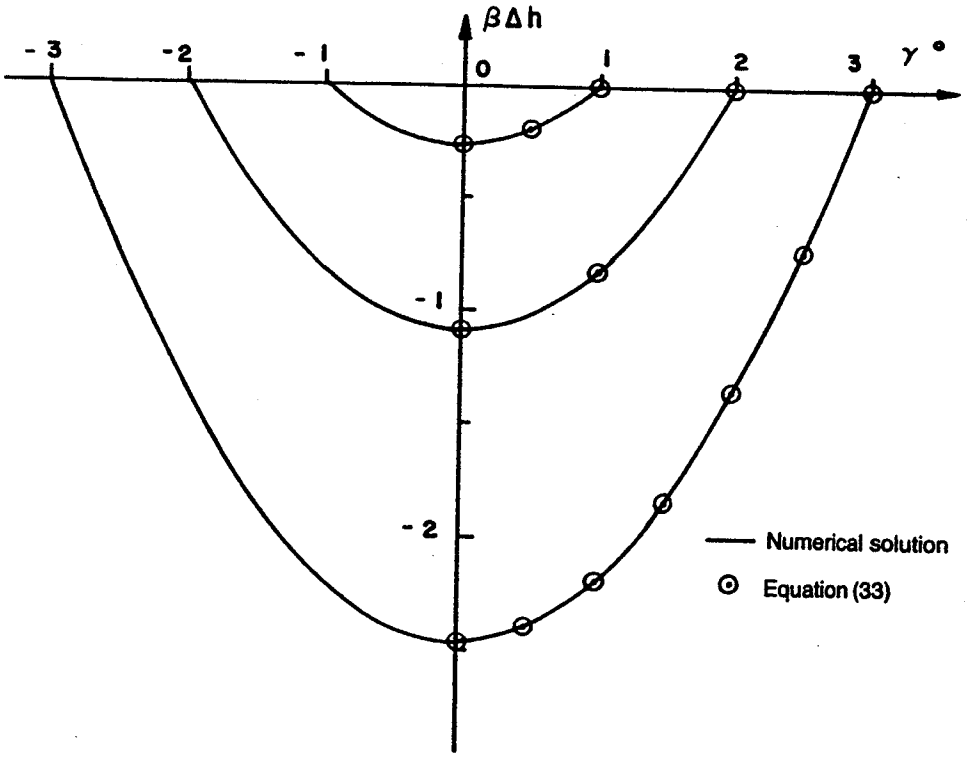

FIG. 2. Ballistic Skip Trajectories with Parabolic Entry at Small Angles. Case of $\varepsilon = 0.0005$.

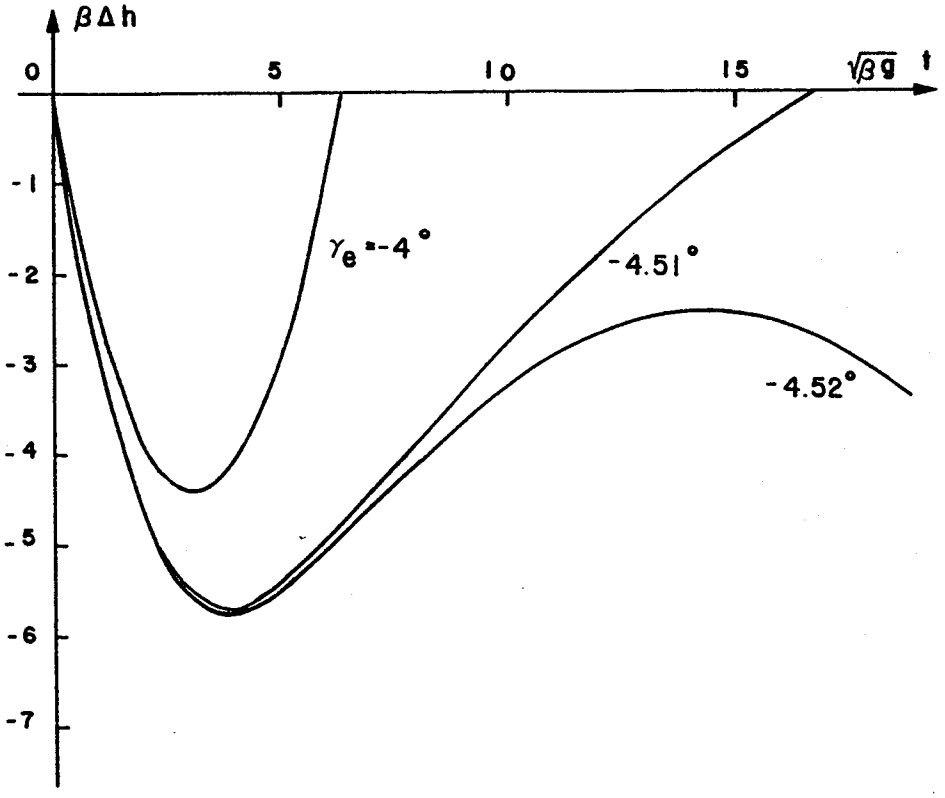

FIG. 3. Ballistic Skip Trajectories with Parabolic Entry at Large Angles. Case of $\varepsilon = 0.0005$.

family of parabolas. If the second-order solution is used, for the case of $\gamma_e = -3°$, the difference in linear altitude is less than 50 meters at the exit point.

At larger entry angles, there is a drastic change in the behavior of the trajectory. This is shown in Fig. 3, which plots the variations of the dimensionless altitude as a function of the dimensionless time, $(\beta g)^{1/2}t$. The critical entry angle γ_e^* is between the values $-4.51°$ and $-4.52°$. The sensitivity of the trajectory near this critical value is obvious. While at $\gamma_e = -4.51°$, the vehicle still exits at an angle $\gamma_f = 0.545°$; by increasing $-\gamma_e$ by one-hundredth of a degree, the vehicle fails to exit while reaching a maximum altitude at a point 20 km below the top of the sensible atmosphere. The effect is due to the larger drag force along a lower trajectory.

Figure 4 presents the variations of the flight path angle as a function of the speed variable τ. Along a skip trajectory with small entry angle, the flight path angle monotonically increases, with γ_f slightly less than the absolute value of γ_e, as shown in the figure for the case where $-\gamma_e \leq 4°$. When the entry angle γ_e approaches its critical value γ_e^*, the exit angle decreases rapidly to grazing exit, $\gamma_f = 0$. When $-\gamma_e \leq 3°$, the second-order solution is nearly identical to the numerical solution. At larger entry angles the second order solution has a limitation which reduces its range of application. This is because for the analytic solution, by virtue of equation (35), the variable τ has an asymptotic value when the error function becomes unity, and the solution cannot be extended beyond this value. As a rule, the second order solution can be used for trajectories with an entry angle up to one degree away from the critical entry angle. For the case of entry angles near the critical value, we shall derive in the following section an alternate solution in equation (62). This solution is shown in small circles in Fig. 4.

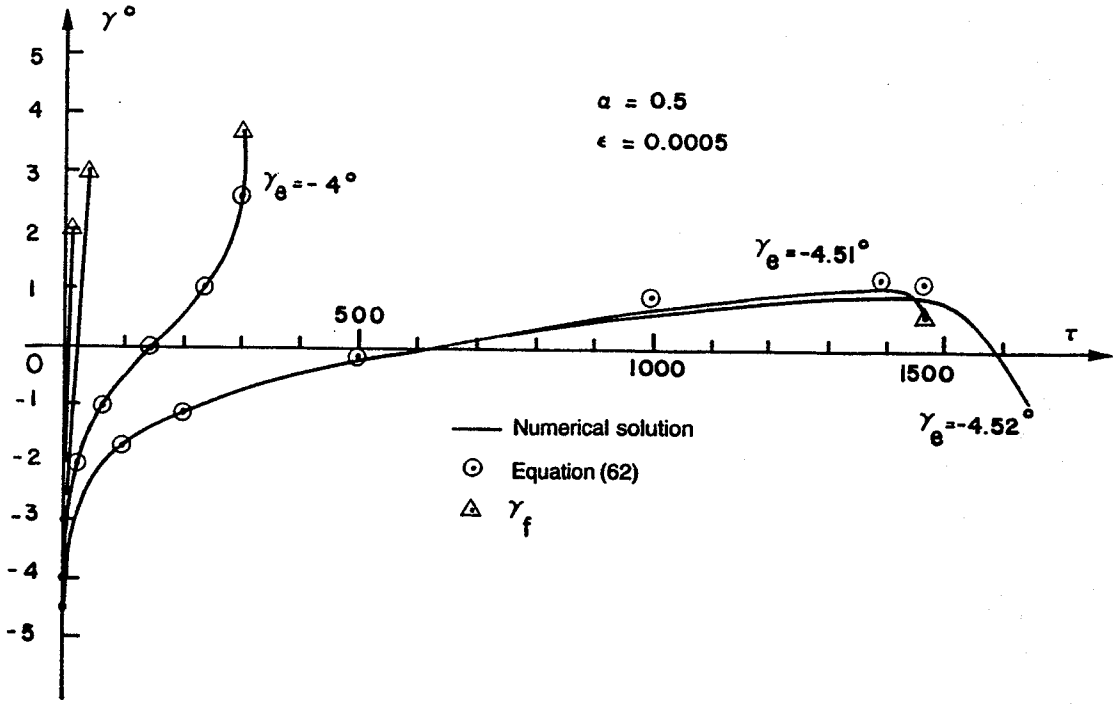

FIG. 4. Variation of the Flight Path Angle as a Function of the Speed Variable.

In general, for all entry angles up to the critical value γ_e^*, the second-order solution is accurate up to the lowest point of the trajectory. This is sufficient for the computation of the peak heating rate and the peak deceleration, since they both occur during the descent. To make this behavior more explicit, we have plotted in Fig. 5 the deceleration as given by equation (19) for the case of a rather large entry angle, $\gamma_e = -4°$. The second-order solution is used, with ϕ_0 as the independent variable, which decreases from the initial value $c = 2.09$ down to $\phi_0 = -1$. At this point the speed variable τ [as computed from equation (35)] has reached 92 percent of its asymptotic limit, and to finish the plot we have used the alternate solution [equation (62)]. The figure shows an excellent agreement between the analytic solution and the numerical solution.

To obtain the point of maximum deceleration from equation (20) which expresses the stationary condition for the function a/g, we use the first order solution to write

$$\phi_0 + \varepsilon\phi_1 = \varepsilon y_0 + \varepsilon^2 y_1 \tag{51}$$

It is clear that ϕ_0 is small and from the zeroth and the first-order solutions, we take approximately at this point

$$y_0 = \exp(c^2/\delta), \qquad \tau = (\pi/\delta)^{1/2} y_0 \operatorname{erf}(c\delta^{-1/2}) \tag{52}$$

$$k = (1 - \alpha)\tau, \qquad \phi_1 = \alpha\delta^{-1}k\tau y_0^{-1} + \alpha\delta^{-1}y_0 = \alpha\delta^{-1}y_0[1 + (\pi/2)\operatorname{erf}^2(c\delta^{-1/2})] \tag{53}$$

$$y_1 = 2\alpha\delta^{-2}k y_0 = \alpha\delta^{-3/2}\pi^{1/2} y_0^2 \operatorname{erf}(c\delta^{-1/2}) \tag{54}$$

By substituting into equation (51), we have explicitly for ϕ_0

$$\phi_0 + \varepsilon\alpha\delta^{-1}[1 + (\pi/2)\operatorname{erf}^2(c\delta^{-1/2})]y_0 = \varepsilon y_0 + \varepsilon^2\alpha\delta^{-3/2}\pi^{1/2} y_0^2 \operatorname{erf}(c\delta^{-1/2}) \tag{55}$$

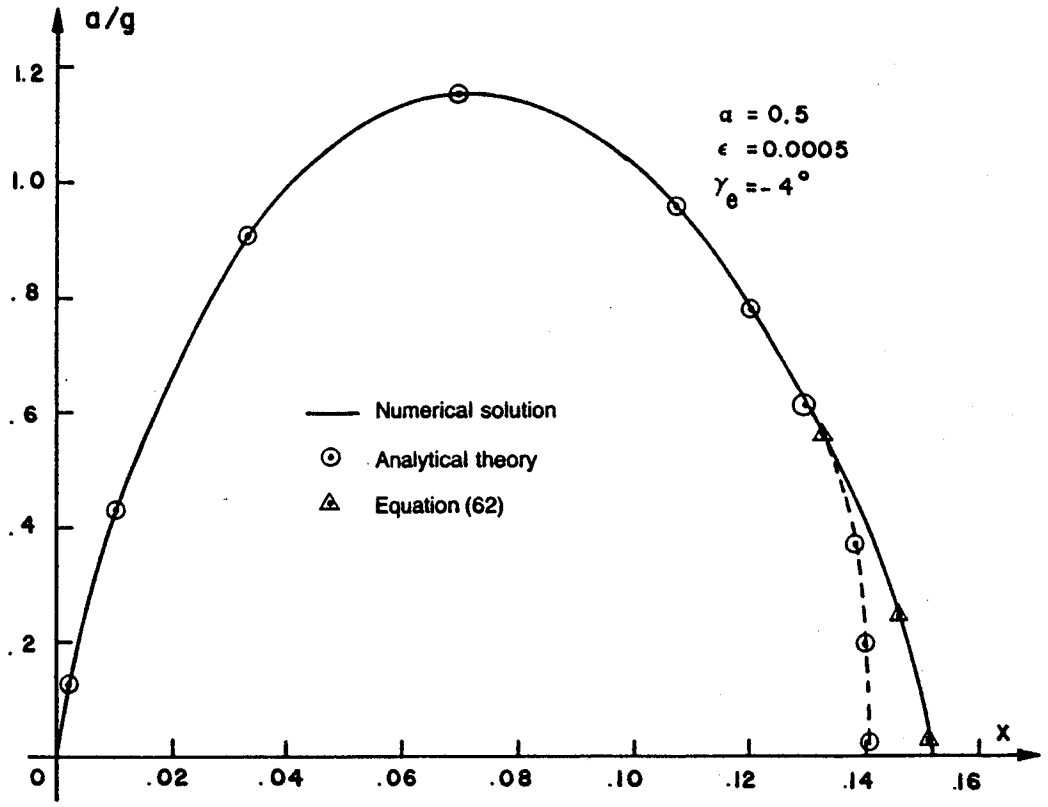

FIG. 5. Variation of the Deceleration along a Ballistic Skip Trajectory.

where, of course, y_0 is given by the first of equations (52) as a function of c. Once this value of ϕ_0 (which is near zero) has been computed the value of ϕ (which is positive) and the normalized density y at the point of maximum deceleration can be obtained using the second-order theory. Using the first order solution and taking $\phi_0 \approx 0$, we have the useful formula for the flight path angle at the point of maximum deceleration

$$\phi = \varepsilon\alpha\delta^{-1} \exp(c^2/\delta)[1 + (\pi/2)\,\mathrm{erf}^2(c\delta^{-1/2})] \tag{56}$$

which displays the various effects of entry angle, entry speed, and ballistic coefficient on this critical flight path angle.

To assess the influence of the ballistic coefficient on exit conditions, equations (15) have been integrated numerically with $\alpha = 0.5$ for parabolic entry and with various entry angles, while two values of the ballistic coefficient, $\varepsilon = 0.0001$ and 0.0025, are selected for the two families of trajectories generated. As expected, the behavior of the ballistic skip trajectory remains the same as for $\varepsilon = 0.0005$. For the case of low ballistic coefficient, $\varepsilon = 0.0001$, the critical angle γ_e^* is between the values $-5.12°$ and $-5.13°$, while for the case of high ballistic coefficient, $\varepsilon = 0.0025$, it is between the values $-3.81°$ and $-3.82°$. Again, a difference of one-hundredth of a degree changes the trajectory from skip to crashing. This shows the desirability of having some thrusting mode near exit to guide the trajectory along the desired flight path.

Figure 6 is a plot of the exit angle γ_f versus the negative of the entry angle γ_e for the three values of the ballistic coefficient. It is seen that the influence of ε is slight at low entry angle, since the exit angle is practically the negative of the entry angle, as given by the zeroth order solution. The primary effect of high drag coefficient is in

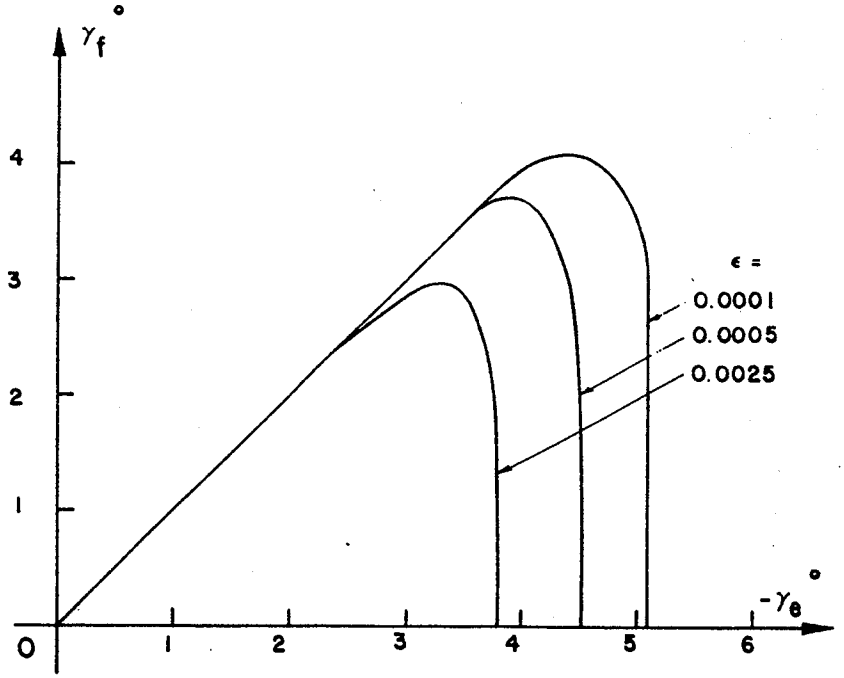

FIG. 6. Exit Angle as a Function of the Entry Angle for Different Values of Ballistic Coefficient. Case of Parabolic Entry.

reducing the exit speed and in lowering the absolute value of the critical angle γ_e^*. Large wing loading, that is, a high value of mg/S, has the opposite effect. The effect of ε on exit speed is obvious from equation (50).

Finally, the effect of entry speed is considered by varying the value of the speed parameter α. With $\varepsilon = 0.0005$, we now take the value $\alpha = 0.577$, which corresponds to an entry speed for a return from a geosynchronous orbit. From the zeroth order solution, at the lowest point of the trajectory

$$y_{max} = \exp(c^2/\delta) \tag{57}$$

and at the exit point, when the entry angle is not near the critical angle,

$$\tau_f = 2(\pi/\delta)^{1/2} \exp(c^2/\delta)\ \mathrm{erf}(c\delta^{-1/2}) \tag{58}$$

Hence, the lower entry speed (that is, a lower value of δ) for the same value of entry angle, the lowest altitude is smaller and the exit speed ratio V_f/V_e is also smaller. Low entry speed also reduces the absolute value of the critical angle γ_e^*. This fact will be made explicit in the following analysis.

The speed ratio, V_f/V_e, as a function of the entry angle, is presented in Fig. 7 for the two cases of parabolic entry and return from geosynchronous orbit. The analytic solution is also plotted in the graph. At low entry angle it is accurate to use the zeroth order solution as given in equation (58). Near the critical angle, however, an alternative equation, derived below, has to be used.

Trajectory Near the Critical Angle

As seen in Fig. 4, for a skip trajectory with shallow entry angle, the flight path angle monotonically increases from a negative value to a positive exit value which is slightly

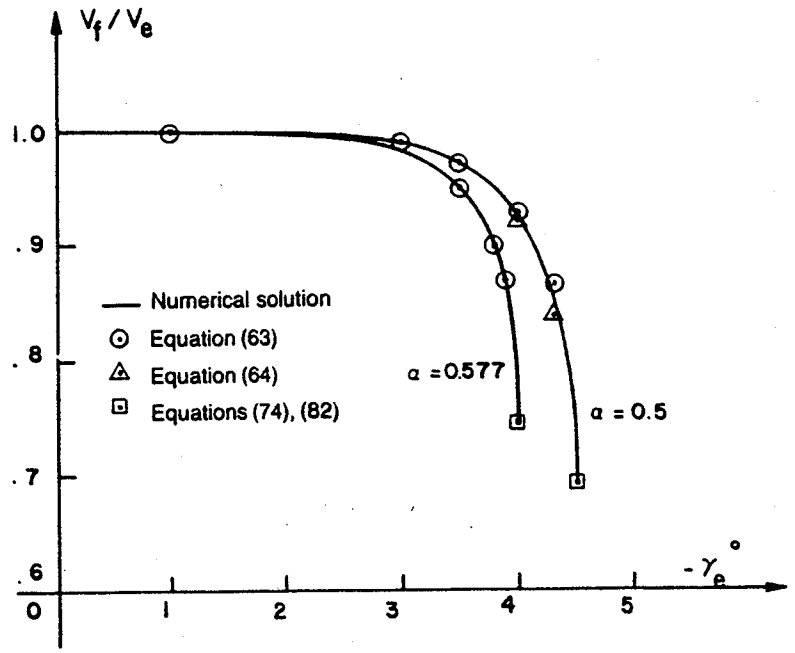

FIG. 7. Effect of Entry Angle and Entry Speed on Exit Speed Ratio. Case of $\varepsilon = 0.0005$.

less in absolute value than the entry value. As the entry angle becomes steeper, approaching the critical value γ_e^*, after passage through the minimum altitude, where $\gamma = 0$, the flight path angle increases to a maximum and then decreases again to zero, when the vehicle reaches the maximum altitude. If this maximum altitude is inside the atmosphere, the vehicle fails to exit. At the point of maximum flight path angle, the trajectory exhibits an inflection point. To account for this behavior, we return to the original system, equations (11) and (12), to obtain the speed variable at the inflection point

$$x_i = -\log \alpha \tag{59}$$

From the definitions of x and α, it is seen that this corresponds to circular speed.

For the critical trajectory, $\gamma_e = \gamma_e^*$, $\gamma_f = 0$, it is obvious that the final speed variable x_f is larger than this value. This means that the exit speed is subcircular. To have the correct behavior of the flight path angle near the critical case, we use the zeroth order solution,

$$Z = \varepsilon y = \varepsilon \exp[(c^2 - \phi^2)/\delta] \tag{60}$$

in equation (12) to have approximately

$$\varepsilon \exp[(c^2 - \phi^2)/\delta]\, d\phi = (\alpha e^x - 1)\, dx \tag{61}$$

We notice that the approximate function ϕ, obtained by the analytical integration of this equation, passes through its stationary value at exactly the same speed as the exact solution obtained through numerical integration. Hence, using this scheme, the analytical solution for ϕ expressed as a function of the speed variable x displays the correct behavior of the flight path angle. This flight path angle is slightly larger than the exact value, due to the approximation in altitude as given in equation (60). Upon

integrating equation (61) we have the following relation between the flight path angle and the speed.

$$(\varepsilon/2)(\delta\pi)^{1/2}\exp(c^2/\delta)[\operatorname{erf}(c\delta^{-1/2}) - \operatorname{erf}(\phi\delta^{-1/2})] = x + \alpha(1 - e^x) \quad (62)$$

This formula has been verified numerically, and the results are shown in Fig. 4. Up to the value $\gamma_e = -4°$, the results are in excellent agreement with the numerical solution. At higher entry angles, the approximate formula shows a slightly higher value of flight path angle, but its usefulness is evident since it is applicable to the case of near critical entry, as shown in the figure for the case where $\gamma_e = -4.51°$.

The final speed is given in equation (50) by the final value x_f. Theoretically, it is obtained from $y(\tau_f) = 1$, but an approximate estimate is obtained as follows. If the zeroth order solution is used, then we have equation (58) rewritten here in terms of x for convenience as

$$x_1 = 2\varepsilon(\pi/\delta)^{1/2}\exp(c^2/\delta)\operatorname{erf}(c\delta^{-1/2}) \quad (63)$$

However, this only represents a lower bound since the zeroth order solution for the altitude is always higher than the actual altitude; that is, at the speed x_1 the vehicle is still inside the atmosphere and as a consequence $x_1 < x_f$.

On the other hand, if equation (62) is used with subscript 2 for the condition at exit, as mentioned above, we always have $c > -\phi_2 > -\phi_f$. Hence, using $\phi = -c$ in this equation, we have a value x_2 which represents an upper bound, $x_f < x_2$, for the final speed. The equation giving x_2 is

$$\varepsilon(\delta\pi)^{1/2}\exp(c^2/\delta)\operatorname{erf}(c\delta^{-1/2}) = x_2 + \alpha(1 - e^{x_2}) \quad (64)$$

comparing the last two equations, we have the relations between the two bounds

$$(1 - \alpha)x_1 = x_2 + \alpha(1 - e^{x_2}) \quad (65)$$

In summary, since the speed ratio decreases as the speed variable increases, we have the bounds

$$e^{-x_2/2} < V_f/V_e < e^{-x_1/2} \quad (66)$$

For a prediction of the final speed, with a given ballistic coefficient ε, entry speed α, and entry angle c, the values x_1 and x_2 are obtained from equations (63) and (64), respectively. At high entry speed and small entry angle, the values are close to each other and yield an accurate prediction for the speed ratio. At higher entry angle the speed ratio is closer to the lower bound, and we have the approximation $x_f \approx x_2$. We notice that for given values of ε, α and c the value x_1 can always be evaluated from equation (63). On the other hand, since the right-hand side of equation (64) is maximized when $x_2 = -\log\alpha = x_i$, we can only solve for x_2 when the left-hand side of this equation is less than the maximum value of the right-hand side (which equals $\alpha - 1 - \log\alpha$). This method of final speed prediction has been tested numerically for a variety of skip trajectories and the results are shown in Fig. 7 for the two cases of parabolic entry and return from geosynchronous orbit with a ballistic coefficient $\varepsilon = 0.0005$. At low entry angle, we use the solution $x_f \approx x_1$, while at high entry angle we have the approximate solution $x_f \approx x_2$.

While the second-order theory, which is obtained from a rigorous technique of integration, provides excellent results for the speed, altitude and flight path angle relationships, it is restricted to the case of small x_f. Concerning the accuracy of the prediction of the final speed, it is possible to assess this restriction based on equations (65) and (66).

Let V_f be the unknown exit speed and ΔV_f be the absolute value of the error incurred using the analytic solution. Let us assume that we require the accuracy

$$\Delta V_f / V_f = n - 1 \tag{67}$$

where n is a certain prescribed number, close to unity, i.e., $n = 1.005$. To achieve this accuracy, based on the bounds as given in the inequalities (66), it is easy to show that we must have conservatively

$$x_2 - x_1 = 2 \log n \tag{68}$$

By substituting into equation (65), we have the equation for the limiting value of x_1, which only depends on the entry speed

$$n^2 e^{x_1} - x_1 = 1 + (2/\alpha) \log n \tag{69}$$

As an example, with $n = 1.005$, for parabolic entry, $\alpha = 0.5$, we have the limit $x_1 = 0.128022$. From equation (68), the upper bound is $x_2 = 0.137997$. At these limiting values, the speed ratio at exit is such that

$$0.933328 < V_f / V_c < 0.937995 \tag{70}$$

Hence the desired accuracy is achieved. Of course, for lower values of x_1, we have better accuracy in prediction. It should be noticed that the limiting value of x_1 obtained is valid for the whole family of parabolic entries with the accuracy n. It means that any combination of ballistic coefficient and entry angle considered must give a value x_1, from equation (63), less than the limiting value to have the required accuracy. For example, by taking $\epsilon = 0.0005$, $\gamma_e = -3°$, for parabolic entry, we have from equations (63) and (64), $x_1 = 0.020303$ and $x_2 = 0.020515$. The value x_1 is much less than the limiting value and the prediction for the final speed is within the desired accuracy. As a matter of fact, for this case, the numerical solution gives $x_f = 0.020485$ and hence

$$0.989795 < V_f / V_c = 0.989810 < 0.989900 \tag{71}$$

What remains is the prediction of the critical angle, γ_e^*, for grazing exit, $\gamma_f = 0$, and as a consequence, the smallest exit speed, V_f^*, along this trajectory. This is obviously a difficult task due to the sensitivity which has been displayed through numerical analysis.

First, due to the inflection point, which must occur for grazing exit, we have the condition $x_f^* > x_i = -\log \alpha$. Hence, we have the condition, valid for all trajectories with an inflection point,

$$V_f < \alpha^{1/2} V_c = V_c \tag{72}$$

which gives an upper bound for the critical exit speed. Next, based on equation (62), along the critical trajectory (that is, with $c = c^*$) and at the point before exit where the flight path angle is maximized (that is, when $x = -\log \alpha$), we have

$$(\varepsilon/2)(\delta\pi)^{1/2}\exp(c^2/\delta)[\mathrm{erf}(c\delta^{-1/2}) + \mathrm{erf}(|\phi_{min}|\delta^{-1/2})] = \alpha - 1 - \log\alpha \qquad (73)$$

If the value $\phi_{min} = -(\beta R)^{1/2}\sin\gamma_{max}$ is known, we can solve for the value $c = c^*$. Since the error function is near unity, and along the critical trajectory, the point of maximum γ occurs slightly before exit, at about 1°, and due to the fact that equation (62) overestimates the flight path angle, we take the empirical value 1.67 for the sum of the error functions in equation (73) to have

$$0.835\varepsilon(\delta\pi)^{1/2}\exp[(c^*)^2/\delta] = \alpha - 1 - \log\alpha \qquad (74)$$

The critical angle γ_e^*, according to this formula, is plotted in Fig. 8 versus the drag parameter ε for several values of the entry speed, from parabolic entry, $\alpha = 0.5$, to near circular entry, $\alpha = 0.9$.

In the figure, the small circles denote the cases which have been verified numerically. As expected, high ballistic coefficient decreases the magnitude of the critical angle. Low speed entry also has the same effect. These behaviors are displayed explicitly in equation (74). Furthermore, over a large range of values of α and ε, this formula predicts the critical angle to within one-hundredth of a degree and hence within the sensitivity of the numerical analysis.

As for the smallest exit speed, the appearance of the inflection point near the top of the sensible atmosphere, along the critical trajectory, is always close to grazing exit. At that altitude the rate of decrease in speed is small, and for all practical purposes we can use the empirical formula

$$V_f^* = 0.98\,\alpha^{1/2}V_e \qquad (75)$$

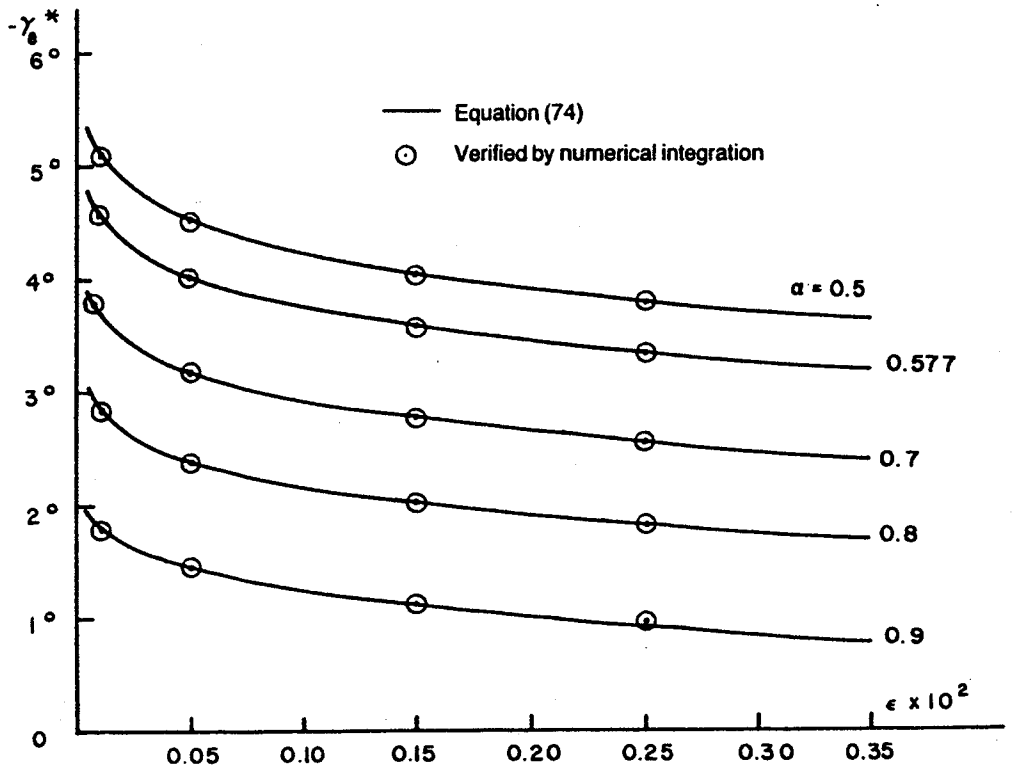

FIG. 8. Variation of Critical Angle as a Function of Ballistic Parameter.

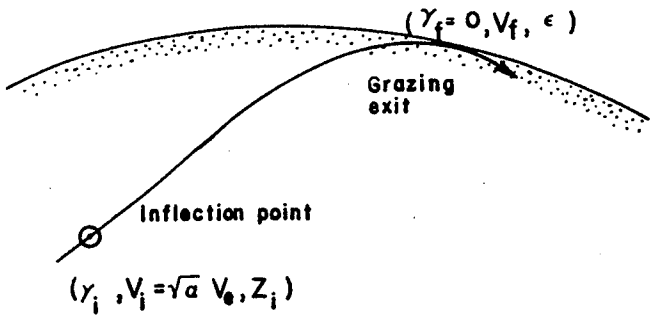

FIG. 9. Grazing Exit Trajectory.

To have a more rigorous assessment of this speed, we consider Fig. 9 which shows the critical trajectory for grazing exit.

We shall attempt an analytical integration of equations (11) and (12) between the inflection point and the exit. As shown in the figure, with the partial knowledge of the end conditions, this amounts to solving a two-point boundary value problem if either the flight path angle, γ_i, or the density Z_i at the inflection point is known. It has been found through extensive numerical analysis that at the inflection point the altitude depends strongly on the ballistic coefficient ε, while the flight path angle is always near 1°. This is because at that point, the flight path angle is stationary, and then decreases over a small variation in the speed to the final value zero. With numerical data for a large number of skip trajectories we take the average values

$$\gamma_i = 0.7°, \qquad \phi_i = -(\beta R)^{1/2} \sin \gamma_i \tag{76}$$

Let Δx be the speed increment beyond the inflection point

$$x = x_i + \Delta x = -\log \alpha + \Delta x \tag{77}$$

Then, for small Δx, we write equations (11) and (12) as

$$dZ/d\,\Delta x = \phi \tag{78}$$

$$d\phi/d\,\Delta x = \Delta x/Z \tag{79}$$

We integrate equation (78) by using an average value for ϕ, taken as the value at the inflection point. This approximation is correct since between the inflection point and the grazing exit, most of the speed depletion occurs at the lower part of the trajectory. Then, we have the linear approximation for the variation of the density

$$Z = Z_i + \phi_i\, \Delta x \tag{80}$$

Upon substituting into equation (79) and integrating between γ_i and zero, we have the relation

$$y_i(\log y_i - 1) = -1 - \phi_i^3 \varepsilon^{-1} \tag{81}$$

With the estimated value of ϕ_i as given in equation (76), this equation can be solved for y_i, that is, for the altitude at the inflection point. Its dependence on the ballistic coefficient ε is clear from the equation. The altitude at the inflection point is lower with lower ballistic coefficient. The speed increment between the inflection point and the exit is obtained from equation (80) as

$$\Delta x = -\varepsilon(y_i - 1)/\phi_i \tag{82}$$

The last points on the curves in Fig. 7 are computed using equation (74) for the flight path angle and equations (81) and (82) for the speed. The estimate for the speed is slightly smaller than the numerically computed speed. Hence, it constitutes a lower bound for equation (72). Due to the sensitive nature of the critical trajectory, other attempts for an improvement of the accuracy have not been successful.

Conclusions

In this paper we have derived a generalized Yaroshevskii system of equations for analyzing ballistic skip trajectories at supercircular entry speeds. Using Poincaré's method of small parameters, a second-order analytical solution has been obtained which for small entry angles shows excellent agreement with the numerical solution.

The analytic solution displays explicitly the influence of the ballistic coefficient, entry speed and entry angle on exit conditions. At higher entry angles, near a critical angle where the vehicle fails to exit, the trajectory exhibits an inflection point where the flight path angle is stationary. This critical trajectory is analyzed in detail, and analytic formulas are obtained for the prediction of the critical angle, the altitude of the inflection point and the smallest exit speed in terms of the ballistic coefficient and the entry speed. The results obtained are useful for an in-depth understanding of a ballistic skip trajectory, which constitutes an important phase in the problem of planetary aerogravity capture and the problem of aeroassisted orbital transfer.

Acknowledgments

Part of the research described in this paper was supported by the Jet Propulsion Laboratory, California Institute of Technology, under contract No. 956416.

References

[1] WALBERG, G. D. "A Review of Aeroassisted Orbit Transfer," AIAA Paper No. 82-1378, AIAA 9th Atmospheric Flight Mechanics Conference, San Diego, California, August 1982.

[2] KECHICHIAN, J. A., CRUZ, M. I., VINH, N. X., and RINDERLE, E. A. "Optimization and Closed-Loop Guidance of Drag-Modulated Aeroassisted Orbital Transfer," AIAA Paper No. 83-2093, AIAA 10th Atmospheric Flight Mechanics Conference, Gatlinburg, Tennessee, August 1983.

[3] VINH, N. X., BUSEMANN, A., and CULP, R. D. *Hypersonic and Planetary Entry Flight Mechanics*, The University of Michigan Press, 1980.

[4] YAROSHEVSKII, V. A. "The Approximate Calculation of Trajectories of Entry into the Atmosphere," Part I, Translated from *Kosmicheskie Issledovaniya*, Vol. 2, No. 4, 1964.

[5] LONGUSKI, J. M., and VINH, N. X. "Analytic Theory of Orbit Contraction and Ballistic Entry into Planetary Atmospheres," Jet Propulsion Laboratory, Pasadena, California, September 1980.

[6] ABRAMOWITZ, M., and STEGUN, I. A. *Handbook of Mathematical Functions*, Dover Publications, Inc., New York, 1972.